Development of Therapeutic Gramicidin S Analogues Bearing Plastic β,γ-Diamino Acids

Qinkun Guan, Kaisen Chen, Qiang Chen, Jianguo Hu, Keguang Cheng, Chengfei Hu, Jibao Zhu, Yi Jin, Emeric Miclet, Valérie Alezra, et al.

Development of Therapeutic Gramicidin S Analogues Bearing Plastic β,γ-Diamino Acids

Qinkun Guan,[a]# Kaisen Chen,[b]# Qiang Chen,[b] Jianguo Hu,[c] Keguang Cheng,[d] Chengfei Hu,[a] Jibao Zhu,[a] Yi Jin,[a] Emeric Miclet,[e] Valérie Alezra,[f] Yang Wan[a][d][f] *

[a] Q. Guan, C. Hu, J. Zhu, Prof. Dr. Y. Jin, Dr. Y. Wan
National Pharmaceutical Engineering Center for Solid Preparation in Chinese Herbal Medicine
Jiangxi University of Traditional Chinese Medicine
1688 Meiling Avenue, WanLi, Nanchang 330004, P. R. China
E-mail: wy15506@gmail.com

[b] Prof. Dr. K. Chen, Q. Chen
Department of clinical laboratory
The First Affiliated Hospital of Nanchang University
17 Yongwaizheng Street, Donghu, Nanchang 330006, P. R. China

[c] Dr. J. Hu
College of Pharmacy
Jiangxi University of Traditional Chinese Medicine
1688 Meiling Avenue, WanLi, Nanchang 330004, P. R. China

[d] Prof. Dr. K. Cheng, Dr. Y. Wan
State Key Laboratory for Chemistry and Molecular Engineering of Medicinal Resources
Guangxi Normal University
15 Yuchai Road, Guilin 541004, P. R China

[e] Prof. Dr. E. Miclet
Laboratoire des Biomolécules
Sorbonne Université, PSL University, CNRS
4 Place Jussieu, Paris F-75005, France

[f] Prof. Dr. V. Alezra, Dr. Y. Wan
Laboratoire de Méthodologie, Synthèse et Molécules Thérapeutiques (ICMMO)
Université Paris-Sud, UMR 8182, CNRS, Université Paris-Saclay
Bât 410, Facultédes Sciences d'Orsay, Orsay, 291405, France

# These authors contributed equally to this work.

Abstract: Gramicidin S (GS), one of the most widely investigated antimicrobial peptides (AMPs), is known for its robust antimicrobial activity. However, it is restricted to topical applications due to undesired hemolytic activity. With the aim to obtain non-toxic GS analogues, we describe herein a molecular approach where the native GS β-turn region is replaced by synthetic β,γ-diamino acids (β,γ-DiAAs). Four β,γ-DiAA diastereomers were employed to mimic β-turn structure to afford GS analogues GS**3**-**6** that exhibit diminished hemolytic activity. A comparative structural study demonstrates that the (β*R*,γ*S*)-DiAA displays the most stable β-turn mimic. To further improve the therapeutic index (*e.g.* high antibacterial activity and low hemolytic activity) and to extend the molecular diversity, GS**5** and GS**6** were used as structural scaffolds to introduce additional hydrophobic or hydrophilic groups. We show that GS**6K,** GS**6F** and GS display comparable antibacterial activity while GS**6K** and GS**6F** possess significantly decreased toxicity. Moreover, antibacterial mechanism studies suggest that GS**6K** kills bacteria mainly through the disruption of membrane.

Introduction

Bacterial resistances are increasing while the development of novel antibiotics is declining.[1] In Europe, approximately 25 000 people die every year due to antibiotic-resistant infections.[2] Without urgent measures, we may enter into the 'post-antibiotic' era, in which none of the known antibiotics will be active. In addition to a tight control of the use of the existing antibiotics,[3] there is an urgent need for novel anti-infection agents that possessing alternative mechanism of action to combat antimicrobial resistance.[4] Delightfully, among the new emerging categories of potential antibiotics, antimicrobial peptides (AMPs) are considered to be one of the most promising alternatives to classic antibiotics. Many AMPs are known to display an extraordinarily broad range of antimicrobial activities covering both Gram-positive and Gram-negative bacteria as well as viruses, fungi and tumors.[5] More importantly, it is common knowledge that AMPs kill microorganism through the disruption of lipid bilayers of cell membrane, which makes it very difficult for microorganisms to develop resistance.

Gramicidin S (GS) is an amphiphilic cyclodecapeptide which adopts a rigid C_2-symmetric β-hairpin structure with the primary sequence *cyclo*-(Pro-Val-Orn-Leu-^{D}Phe)$_2$.[6–9] Its strong amphiphilicity results from spatially segregated hydrophobic residues (Val and

Leu) and cationic residues (Orn) in the β-strands. GS was isolated from *Bacillus brevis* in the Soviet Union in 1942 and was primary applied to treat infected wound.[10] There is a general agreement that GS kills bacteria by the disruption of membrane bilayer, though its precise mechanism of action is still debated. Proposed models include the formation of discrete pores or the membrane destruction in a detergent-like manner.[11–16] More recent studies showed that GS can not only induce the disruption of membrane but can also delocalize the peripheral membrane proteins.[13,15] Unfortunately, GS is not selective toward the lipid bilayer which causes severe toxicity towards human erythrocyte.[17] In order to obtain non-toxic GS analogues, GS has been the subject of extensive structure−activity relationship (SAR) studies.[18,19] It has become clear that the biological activity of GS is determined by a panel of physicochemical parameters: cationicity, hydrophobicity, amphiphilicity and hydrophobic aromaticity.[18] In the past decades, many strategies, including ring size variation,[20–22] β-turn modification,[23–30] β-strand modification[31,32] and light-controllable "smart" analogues[33–35] have been recognized as different routes to conceive new potent antimicrobial molecules endowed with low toxicity against human cells. However, to date, there is no clinically applicable antibiotic related to GS and thus a constant investment in this field is required.

Among the molecular approaches, we are particularly interested in the modification of ^{D}Phe-Pro motif in the β-turn region. Several studies have shown that even subtle changes in the β-turn region could have a dramatic impact on the biological profile,[26,27,32,36] suggesting this region is a promising target for modulating GS structure and activity. Both α-amino acids and unnatural dipeptide surrogates have been employed to substitute the native ^{D}Phe-Pro motif.[32,37,38] Interestingly, mimicking the β-turn by unnatural dipeptide surrogates often results in a slight distortion of the cyclic β-hairpin structure and subsequently leads to an optimal amphiphilicity.[26,39]

In our group, we have also contributed in the development of GS-based antibiotics.[18,23] Our strategy involves the replacement of the native GS β-turn ^{D}Phe-Pro by synthetic β,γ-diamino acids (β,γ-DiAAs) that can possess combination of stereochemistry and hydrophilicity/hydrophobicity. We have previously shown that when introduced into short peptides, β,γ-DiAAs are capable to induce stable C_9 or C_{12} intra-molecular H-bonds which finally stabilize well-defined conformations.[40,41] Therefore, β,γ-DiAAs appear very promising to stabilize the β-turn region of GS and in the same time to maintain its global amphiphilic character. The uncoupled second nitrogen of β,γ-DiAA is a source of hydrosolubility or further functionalization, facilitating the stepwise structural optimization. In the last work, we have synthesized a pair of GS analogues GS**1** and GS**2** (**Figure 1**) with β-turn regions disubstituted with β,γ-DiAAs.[23] Both

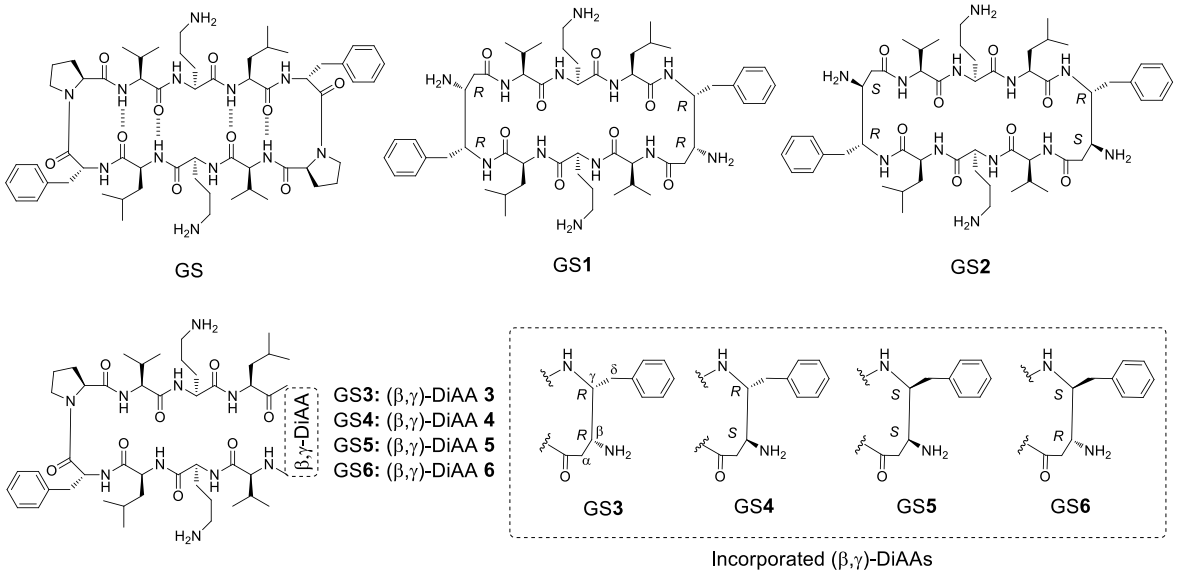

Figure 1. GS and GS analogue **1**-**6** with β-turn region mono- or disubstituted with β,γ-DiAAs

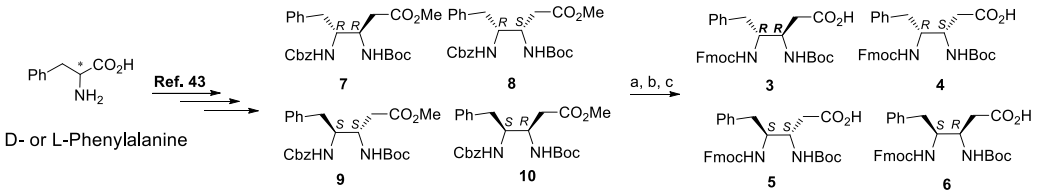

Scheme1. Synthesis of Fmoc-protected β,γ-diAAs. Synthetic conditions: (a) LiOH, H_2O/THF; (b) Pd/C, H_2, MeOH; (c) FmocOSu, K_2CO_3, 1,4-Dioxane/water.

analogues displayed totally diminished hemolytic activity while maintained bactericidal activity against a panel of pathogenic strains. Nevertheless, the conformational features of those analogues weren't discussed in details and their antibacterial activities were weak compared to GS. In this study, we synthesized four additional analogues (GS**3**-**6**, **Figure 1**) with β-turn region monosubstituted by β,γ-DiAA that differing in stereochemistry. After conformational and biological evaluation, GS**5** and GS**6** were selected as molecular scaffolds for further modification to obtain analogues conferred with high therapeutic index. The biological studies demonstrate that GS**6K** and GS**6F** are highly toxic to bacterial strains, but are much less toxic to human blood cells.

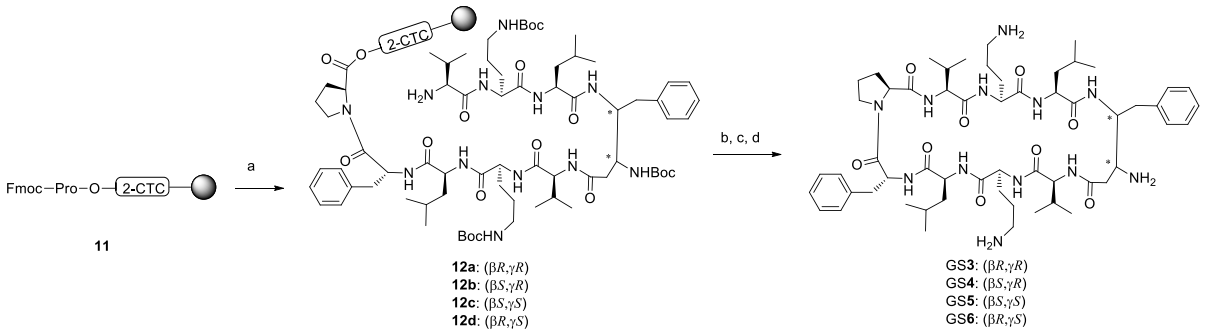

Scheme 2. Synthesis of GS**3**-**6**. (a) Sequential coupling (Xaa or β,γ-DiAA, HBTU, HOBt, DiPEA, DMF) and deprotection (20% piperidine/DMF, v/v) steps; (b) 1% TFA/DCM, v/v, 5x 10 min; (c) PyBOP, HOBt, DiPEA, DMF; (d) 90% TFA/water, v/v.

Results and Discussion

Scope of Lead Peptide

Molecular Design and Synthesis. Initially, four diastereomeric GS analogues (GS**3**-**6**, **Figure 1**) were synthesized to evaluate in both biological and conformational aspects. The β,γ-DiAAs were prepared using the synthetic strategy previously described by our group starting from α-amino acids.[42] With respect to the aromatic character in the β-turn region,[36,39] D- and L-phenylalanine were chosen as starting materials (**Scheme 1**). Cbz-protected intermediates **7**, **8**, **9** and **10** were prepared as previously described.[23,43] Since the configuration of an analogue of compound **9** has been previously determined by crystallographic structure,[43] the other compounds could thereby be differentiated by the comparison of their NMR spectrum with their enantiomers. Noteworthy, the separation of the diastereomers is rather difficult when directly applying the silica gel chromatography. Alternatively, the minor diastereomers (**8** and **10**) can be easily precipitated in the presence of cold diethyl ether, and it consequently allows the major diastereomers (7 and **9)** being purified by chromatography. To allow the solid phase synthesis, Cbz protecting group was further transferred to Fmoc protecting group (**Scheme 1**).

Previous studies have demonstrated that GS and its analogues can be readily synthesized by solution-phase cyclization of the corresponding linear precursor peptides with protected side chains.[44] To this end, the linear precursors were assembled by following an either conventional or microwave-assistant solid phase Fmoc/*t*Bu strategy. All Fmoc-protected α-amino acids are commercially available. Each projected peptide was assembled stepwise on the solid support starting from Fmoc-Pro-2-Chlorotrityl Chloride (CTC) Resin. During the sequential coupling, HBTU/HOBt (conventional synthesis) or HBTU (microwave-assistant synthesis) was used for activation, DiPEA as base, DMF as solvent and 20% piperidine for Fmoc deprotection. Resin cleavage was achieved in the condition of 1% TFA/DCM (v/v) to keep the side-chain protecting groups intact. The subsequent macrocyclization was achieved in diluted solution (2 mg/mL) to lower the hetero-condensation. After global deprotection in the presence of TFA/H_2O (9:1, v/v), crude peptides were pre-purified by the precipitation in the presence of cold diethyl ether and then further purified by reverse-phase high performance liquid chromatography (RP-HPLC, **Scheme 2**).

Antibacterial Activity. With cyclic peptides in hand, we evaluated the antibacterial activity of GS**3**-**6** and GS by determination of the minimal inhibitory concentration (MIC) in a standard screening assay in broth (**Table 1**). A representative set of both Gram-positive and Gram-negative bacterial strains were selected for antibacterial testing. In line with literature,[17] GS exhibits potent activity against Gram-positive strains while less efficacy against Gram-negative ones. In comparison to parent molecule, GS**3**-**6** all show in general less activity in various degrees. GS**5** and GS**6** preserve interesting activity against several strains such as *S. bovis* and *E. faecium* while GS**3** is absolutely inactive against all strains.

Table 1. Antibacterial activity of GS**3**-**6** and GS[a][b]

Peptide	Gram-negative bacteria		Gram-positive bacteria				
	E. coli	*P. aeruginosa*	*S. aureus*	*B. subtilis*	*S. bovis*	*E. faecalis*	*E. faecium*
GS	50	50	3.13	3.13	6.25	6.25	3.13
GS**3**	100	100	100	100	100	100	100
GS**4**	50	50	50	50	50	25	25
GS**5**	50	100	50	100	25	25	12.5
GS**6**	25	50	25	50	12.5	25	25

[a] measured as MIC (μg/mL). [b] 100 μg/mL was the maximal tested concentration.

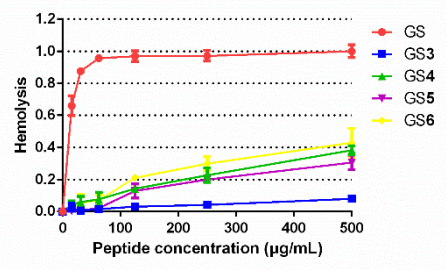

Figure 2. Hemolytic activity of GS**3**-**6** and GS. Percentage hemolysis, mean ± value, and *n* = 3.

Hemolytic Activity. The ability of GS**3**-**6** to lyze human red blood cell was then evaluated in comparison to GS (**Figure 2**). Hemolysis was determined by the exposure of fresh prepared human blood to a range of two-folded peptide concentrations (15.6-500 μg/mL). As it is known,[17] GS induces severe hemolysis in a very low concentration. However, GS**3**-**6** all exert negligible hemolysis in low concentration and the intensity of hemolysis grows slowly as the peptide concentration increases.

NMR Spectroscopy. To learn how the structural variations influence the biological profile, we made a comparative structural study between GS**3**-**6** and GS by NMR spectroscopy in aqueous solution. The complete ^{1}H NMR resonance assignment of each peptide was performed using COSY, TOCSY and NOESY experiments. Large spectral dispersion is observed in HN regions for all peptides except for GS**3** (*See Supporting Information*), suggesting stable conformations form in GS**4**-**6** and GS. As for GS**3**, the observation of overlapped NH signals and the absence of long-range NOE are attributable to the fact that no stable secondary structure is formed. These findings are reminiscent of our previous results that instead of intra-molecular interaction, inter-molecular H-bonds are formed when (β*R*,γ*R*)-DiAA **3** is introduced into short peptides.[45] As can be found in **Table 2**, the ^{3}J CαH-NH coupling constants of the Leu, Orn and Val (ranging between 8.6 and 9.1 Hz) of GS corresponds to a β-sheet structure.[46] A set of comparable values were calculated in GS**6** while not in other analogues, signifying an analogous secondary structure between GS**6** and GS**.** NOESY spectroscopy was also recorded as it is an excellent option for deriving the conformational preferences of cyclic peptides. **Figure 3** shows that the observed long-range NOEs (*e.g.* NH-Leu$_4$ and C$_\beta$H-Val$_7$) in the intact β-turn region of GS**4**-**6** are comparable to that of native GS. Nevertheless, the conformational preferences of the modified region of GS**4**-**6** are significantly distinct. The detected long-range NOEs between NH-Orn$_3$ and C$_\beta$H or C$_\gamma$H of (β*S*,γ*S*)-DiAA in GS**5** indicate a highly bended skeleton conformation, which is consistent with our previous experimental data that multiple H-bonds are formed around (β*S*,γ*S*)-DiAA when it is incorporated into short peptides.[41] On the other hand, the long-range NOEs around β,γ-DiAA residue in GS**4** and GS**6** highlight a C$_9$ H-bond formation between NH-Val$_2$ and CO-Leu$_9$.[40] Overall, GS**6** has a compact β-sheet character which is most likely similar to that of GS.

Table 2. ^{3}J CαH-NH coupling constants (Hz) measured for GS**3**-**6** and GS in 1D ^{1}H NMR spectra recorded in H$_2$O/D$_2$O (9:1, v/v, containing 20 mM PBS buffer) at pH 7.0 and 4 °C.

Peptide	Val$_2$	Orn$_3$	Leu$_4$	^{D}Phe$_5$	Val$_7$	Orn$_8$	Leu$_9$
GS	9.1[a]	9.0	8.6	broad	9.1[a]	9.0	8.6
GS**3**	6.9	6.8	8.2	8.4	5.2	nd[b]	nd[b]
GS**4**	5.6	7.7	8.5	broad	5.6	7.8	nd[b]
GS**5**	6.5	6.5	4.9	nd[b]	6.5	4.5	4.8
GS**6**	8.0	7.2	8.2	broad	7.2	8.3	broad

[a] Measured in 25 °C, data not shown. [b] Not determined because of signal overlapping.

Circular Dichroism (CD) Spectroscopy. To evaluate the content of the secondary structure, CD spectra of GS**3**-**6** and GS were measured in methanol and water (**Figure 4**). In both solvents, the spectral characteristics of GS**3**-**6** are less detectable in comparison to GS. However, GS**6** displays a similar feature to that of GS, albeit the excitation is weaker. Similar to NMR spectroscopy analysis, these experiment data also serves to demonstrate an analogous conformation between GS**6** and GS. The presence of β-sheet and β-turn in the secondary structure are confirmed by the two negative shoulders around 207 and 225 nm.[47] Compared to spectra in methanol, similar spectra characteristics were documented in aqueous solution except an overall attenuation in excitation, highlighting a more induced and stable secondary structure in organic solvent.

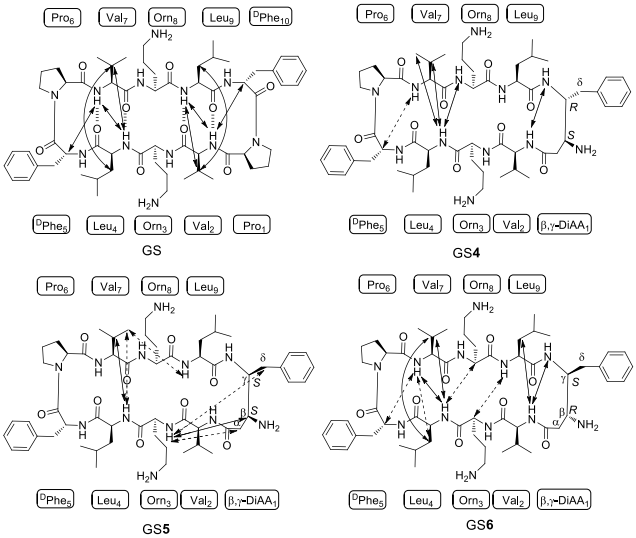

Figure 3. Observed long-range NOEs (mixing time 500 ms) for GS4-6 and GS. Solid double arrows indicate strong NOEs, dotted double arrows indicate weak NOEs. NOESY spectra were recorded in H_2O/D_2O (9:1, v/v, containing 20 mM PBS buffer) at pH 7.0 and 4 °C.

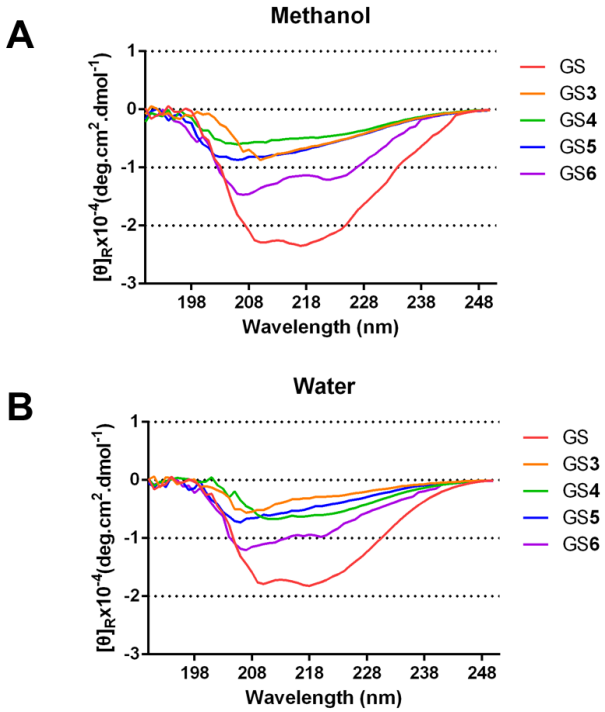

Figure 4. CD spectra of GS**3**-**6** and GS at 0.1 mM in (A) methanol and (B) water.

RP-HPLC Analysis. The estimation of amphiphilic and hydrophobic characteristics of AMPs is interesting as they are highly associated with the biological activities. Since GS**3**-**6** share the same hydrophilic and hydrophobic residues, the difference of biological activities can be partially attributed to the variable amphiphilic characteristics.[48] As an empirical method, the amphiphilicity of GS**3**-**6** were estimated using the RP-HPLC retention times. As shown in **Figure 5**, GS**4**-**6** display ignorable difference with regard to retention time whereas GS**3** has an apparent shorter value. This result signifies that GS**3** possesses a disordered amphiphilic structure, which is line with aforementioned structural studies. When compared to GS, GS**3**-**6** all show much less hydrophobic/amphiphilic content as GS has a greatly extended retention time. It is common knowledge that hydrophobicity of AMPs is closely correlating with hemolytic activity.[47,49] Therefore, the distinction of retention time serves to explain why GS**3**-**6** exhibit significantly reduced hemolytic activity.

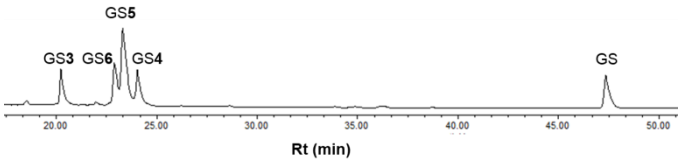

Figure 5. Schematic representation of the retention times observed for GS and GS**3**–**6** on analytical RP-HPLC. Experiments were performed on a Welch XB-C18 column (4.6 x 250 mm, 5 µm) running linear gradients CH_3CN (30-70%) into H_2O (0.1% TFA, v/v) over 60 min at 1 mL/min flow rate, with UV detection at 221 nm.

Development of Further Optimized GS Analogues

Molecular Optimization and Synthesis. Notwithstanding GS**3**-**6** show much decreased hemolytic effect, their bactericidal activities don't meet the demand of clinical application. To improve the therapeutic index and to extend the molecular diversity, further structural optimizations of GS analogues were conducted. Previous studies have demonstrated that the presence of hydrophobic aromaticity in the β-turn region is important to preserve the antibacterial activity[36,39] whereas some others argued that the enhancement of cationicity in the same region may lower the hemolytic activity without hampering the antibacterial activity.[50] We thereby envisioned that tethering additional hydrophobic/aromatic (*e.g.* phenylalanine) or cationic (*e.g.* lysine) residue to the β,γ-DiAA motif may lead to potent GS-related antibiotics endowed with low side effects. Given GS**6** displays the most pronounced β-sheet structure and GS**5** stands for a different type of structural conformation, they were both employed as structural scaffolds for further optimizations (**Figure 6**).

Thanks to the uncoupled second nitrogen in β,γ-DiAA, it allows the introduction of additional group with relative ease. Installation of additional residue in GS**5** or GS**6** can be normally achieved in two strategies: incorporation of 'Fmoc-compatible' functionalized β,γ-DiAA during Fmoc solid phase peptide synthesis or on-resin introduction of functional groups. In our case, the preparation of β-nitrogen functionalized β,γ-DiAA requires a number of protection and deprotection steps which may heavily hamper the efficiency, particularly considering the poor solubility of minor diastereomer (compound **6**) in most organic solvents (except for DMF). For these reasons, the

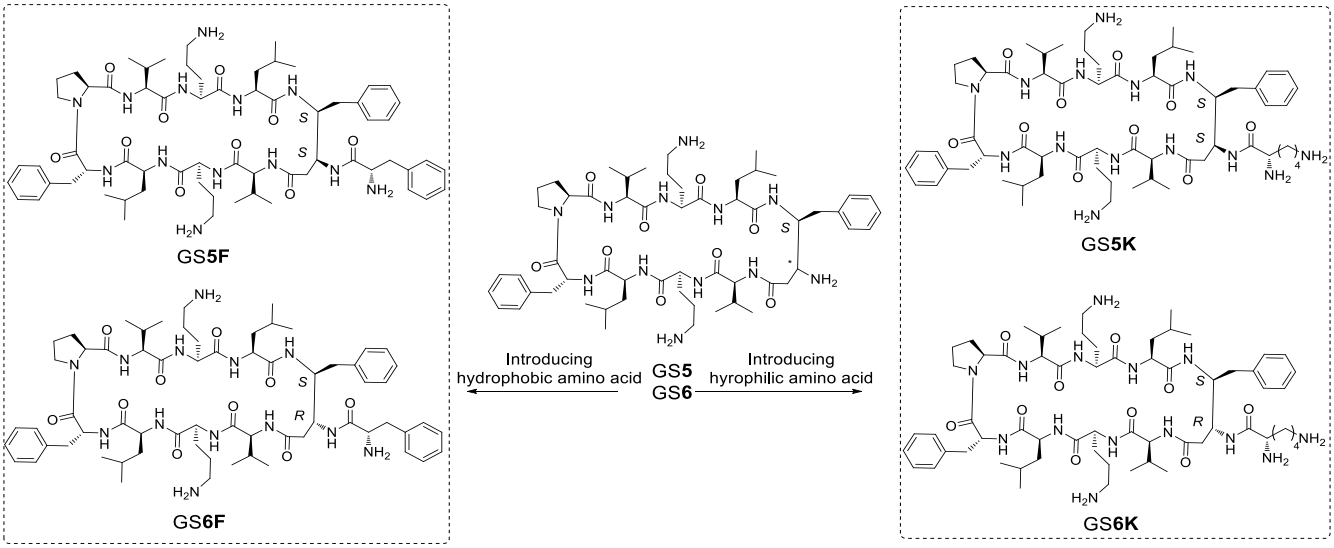

Figure 6. Structure of the further optimized GS analogues.

on-resin introduction of functional groups is a more practical strategy as it simplifies the synthetic procedure and shortens the purification steps. To allow this, Boc protecting group in amino acid **5** or **6** was switched to Alloc protecting group, delivering β,γ-DiAA **5a** and **6a** that are readily for Fmoc solid phase peptide synthesis (**Scheme 3**). The subsequent peptide synthesis followed the aforementioned protocol. After β,γ-DiAA coupling, Alloc group was removed in the presence of $Pd(Ph_3)_4$, followed by the introduction of additional Boc-protected amino acid. Total four analogues GS**5K**, GS**5F**, GS**6K** and GS**6F** were synthesized within reasonable yields (**Scheme 4**).

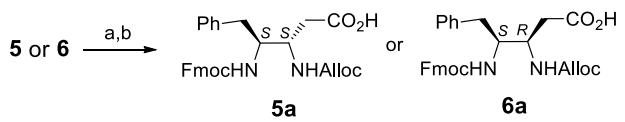

Scheme 3. Synthesis of Alloc-protected β,γ-diamino acids. (a) 50% TFA/DCM, v/v; (b) AllocOsu, Na_2CO_3, 1,4-Dioxane/water.

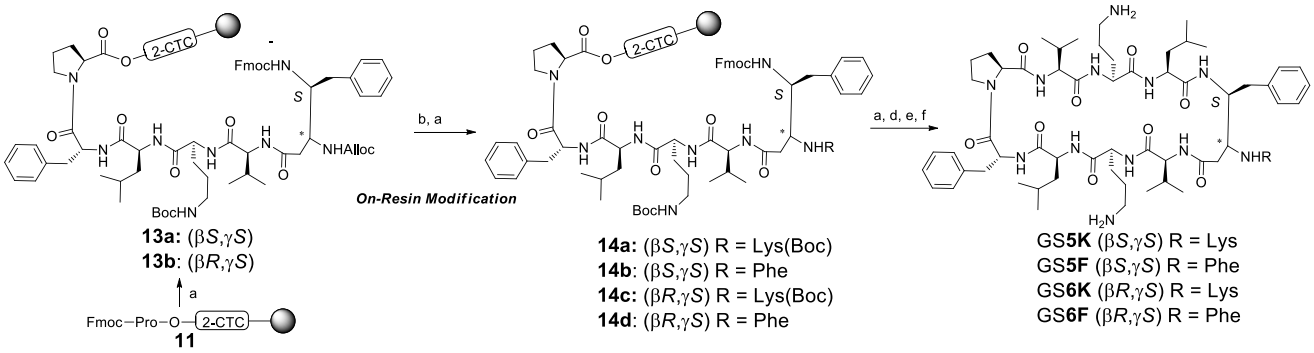

Scheme 4. Synthesis of the further optimized GS analogues. (a) Sequential coupling (Xaa or β,γ-DiAA, HBTU, HOBt, DiPEA, DMF) and deprotection (20% piperidine/DMF, v/v) steps; (b) $Pd(Ph_3)_4$, NMM, AcOH, $CHCl_3$; (d) 1% TFA/DCM, v/v, 5x 10 min; (e) PyBOP, HOBt, DiPEA, DMF; (f) 90% TFA/water, v/v.

Antibacterial Activity. We first tested the antibacterial ability of the newly synthesized GS analogues following the aforementioned protocol. In general, the second batch of GS analogues exhibit superior activity than GS**4**-**6**. Significantly, although differing in molecular approach, both GS**6K** and GS**6F** exerted comparable antibacterial activities against several pathogenic strains (*e.g. S. aureus* and *S. bovis*) to that of native GS (**Table 3**). Presumably, the improved antibacterial activity of GS**6F** is be attributed to the increased aromaticity in β-turn region which favors the π-cation interaction during peptide penetration.[36] On the other hand, the enhancement of cationicity may serve to strengthen the electrostatic interaction between peptide and cell membrane and thus increases the antibacterial ability.[51]

Table 3. Antibacterial activity of the second batch of GS analogues[a][b]

Peptide	Gram-negative bacteria		Gram-positive bacteria				
	E. coli	*P. aeruginosa*	*S. aureus*	*B. subtilis*	*S. bovis*	*E. faecalis*	*E. faecium*
GS	50	50	3.13	3.13	6.25	6.25	3.13
GS**5K**	50	100	25	6.25	12.5	50	12.5
GS**5F**	50	100	25	6.25	12.5	25	12.5
GS**6K**	50	50	12.5	6.25	3.13	12.5	12.5
GS**6F**	50	50	25	3.13	6.25	12.5	12.5

[a] measured as MIC (μg/mL). [b] 100 μg/mL was the maximal tested concentration.

Hemolytic Activity. Next, the hemolytic activities of the second batch of GS analogues were measured. Intriguingly, in spite of the substantially enhanced antibacterial ability occurs, no evident increase of hemolytic activity is gained for all analogues. This is probably due to the maintained or even increased number of cationicity in GS**5F**/GS**6F** and GS**5K**/GS**6K,** respectively**.** In general, all GS analogues display hemolytic activity to a point that is much lower than GS. Having realized both antibacterial and hemolytic profile, GS**6K** was selected as the peptide candidate for further biological studies.

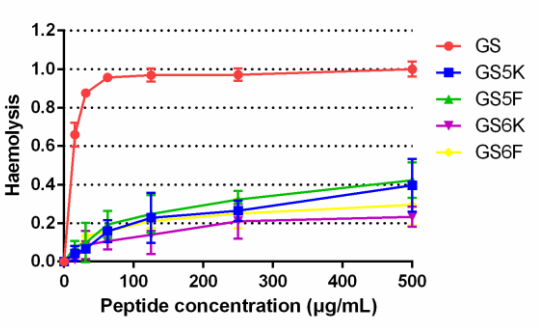

Figure 7. Hemolytic activity the second batch of GS analogues. Percentage hemolysis, mean ± value, and *n* = 3.

Cytotoxicity. Non-toxicity to mammalian cells is also important for the clinical application of AMPs. In this regard, we further evaluated the cytotoxicity of GS**6K** by the determination of cell viability. LO2 cell was used to mimic human liver cell. Cell Counting Kit-8 (CCK-8) assays were carried out in cell medium supplemented with 1% fetal bovine serum. **Figure 8** shows that GS**6K** exerts negligible toxicity towards LO2 cells except for a slightly decrease of cell viability at concentration higher than 10 μM. In contrast, GS displays severe cytotoxicity at low concentration (< 5 μM).

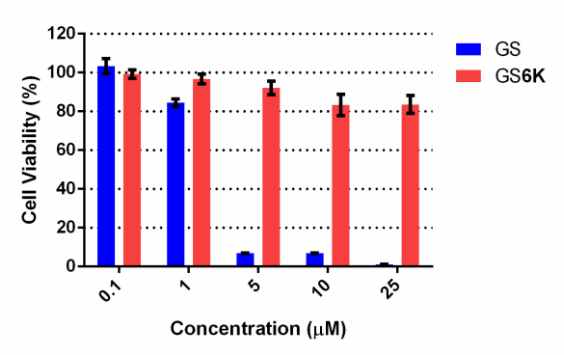

Figure 8. Cytotoxicity of GS**6K** and GS. Percentage cell viability, mean ± value, and *n* = 3

Antimicrobial Mechanism

Cytoplasmic Membrane Depolarization. To understand whether the antibacterial mechanism of the optimum peptide GS**6K** resembles to that of GS, $DiSC_3$-5, a membrane potential sensitive dye, was used to assess bacterial membrane depolarization on *S. aureus* and *B. subtilis*. The distribution of $DiSC_3$-5 between medium and cell membrane is highly depending on the membrane potential. The fluorescence of cationic dye $DiSC_3$-5 is self-quenched when accumulating to cytoplasmic membrane. However, upon membrane disruption, $DiSC_3$-5 is released and resuspended in buffer, leading to fluorescence enhancement. **Figure 9** shows the time course of fluorescence over 30 min. As can be found in **Figure 9**, the addition of GS**6K** (2x MIC) to the medium resulted an immediately increase of fluorescence on both bacterial strains, though the change on *B. subtilis* is less significant. Maximum fluorescence was achieved after addition of GS (4x MIC). These observations suggest that GS**6K** is highly membrane active and behaves similar to that of GS.

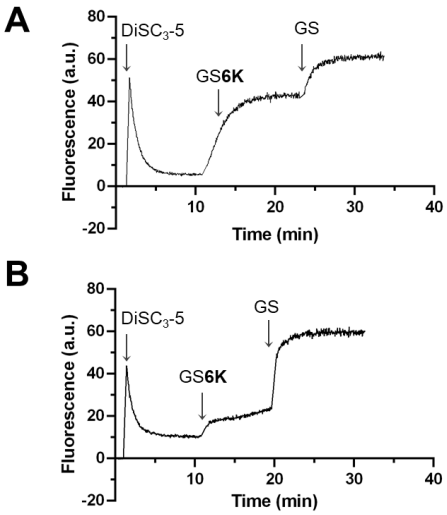

Figure 9. Cytoplasmic membrane depolarization of (A) *S. aureus* and (B) *B.subtilis* by the optimum peptide GS**6K**.

Scanning Electron Microscopy (SEM). To further elucidate the mechanism of action, GS**6K** was used to perform SEM covering both Gram-positive and Gram-negative pathogenic strains. SEM of pathogen cell morphologies is shown in **Figure 10**. Compared to the intact controls (right panel), microbial cells treated with GS**6K** exhibit distinct changes in their morphology (left panel). Unlike the smooth surfaces of the control cells, wrinkled cell walls are observed on *E. faecium* and *S.aureus* cells. While for the rest of bacterial strains, cell membrane was impaired to the point that cell contents leaked out (arrows in **Figure 10**). These results are likely attributable to the fact that GS**6K** kills bacteria through the disruption of cell membrane.

Conclusion

In this work, four diastereomeric GS analogues GS**3**-**6** with β-turn region monosubstituted by synthetic β,γ-DiAAs were

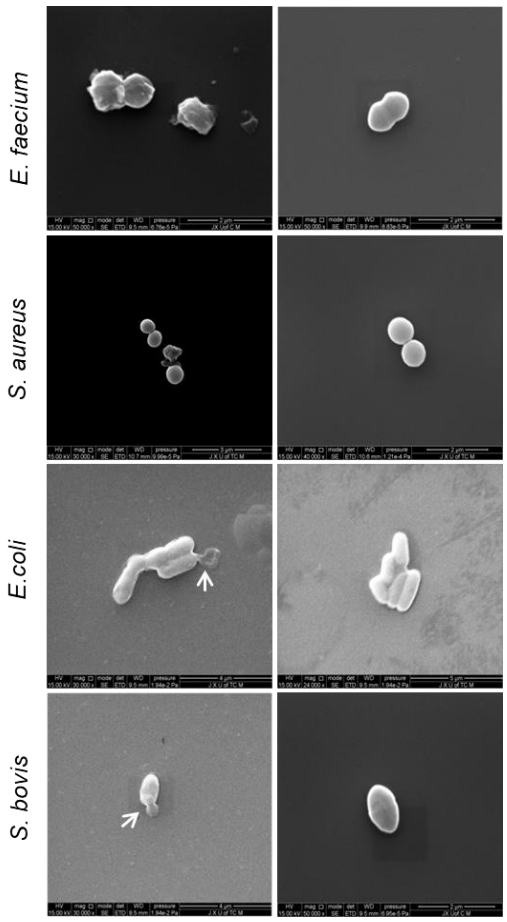

Figure 10. SEM photographs of treated (left panel) and untreated (right panel) bacteria with GS**6K** (2x MIC, 1 h).

primary synthesized to obtain non-toxic GS-based antibiotics. We have shown that (β*R*,γ*S*)-DiAA displays the most stable β-turn mimic among four diastereomers by a comparative structural study. In spite of possessing relatively weak bactericidal activity, GS**3**-**6** all exhibit ignorable hemolytic activities. After introduction of extra hydrophobic or hydrophilic group on β,γ-DiAA motif through on-resin synthesis, we were able to obtain non-toxic peptide GS**6K** and GS**6F** conferred with potent antibacterial activity, highlighting the structural plasticity of our building blocks. $DiSC_3$-5 fluorescence and SEM experiments suggest that the most potent analogue GS**6K** kills bacteria mainly, if not only, through the disruption of cell membrane. This observation is significant as antibiotics possessing such model of action are unlikely to provoke bacterial resistance. It is interesting to find that both **GS6K** and GS**6F** exhibit improved biological profile in comparison to lead peptide GS**6** given the additionally tethered groups encompassing converse physiochemical characters, which highlights the molecular potential of peptide GS**6**. In general, we have shown that it is possible to improve the therapeutic index of GS-based antibiotics by the replacement of ^{D}Phe-Pro motif by a rationally designed β,γ-DiAA. Considering there is virtually no resistance observed for cyclopeptide antibiotics such as gramicidin S and tyrocidines that have been topically applied for over seventy years, it is of great interest to reinvestigate these old but still potent AMPs to combat globally rising bacterial resistance. We hope that our work will encourage and benefit continuous investment in the field of AMP-based drug development.

Experimental Section

General Remarks. Fmoc-Pro-(2-CTC)-resin (1% cross-linked, 100-200 mesh, 0.476 mmol/g) was purchased from GL Biochem (Shanghai) Ltd. DMF was treated with CaH for overnight then distilled under reduce pressure. THF was distilled over sodium/benzophenone under argon. All other reagents and solvents were used without any further purification. Flash chromatography was performed on silica gel (100-200 mesh). Analytical thin-layer chromatography (TLC) was performed using aluminum-backed silica gel plates coated with a 0.2 mm thickness of GF254 silica gel, neutral. ^{1}H, ^{13}C, TOCSY, COSY, HSQC and NOESY spectra were recorded on Bruker AV II 500 or Bruker AV II 600. Chemical shifts are reported in δ units to 0.01 ppm precision with coupling constants reported to 0.1 Hz precision using residual solvent (DMSO-d_6: ^{1}H: 2.50 ppm, ^{13}C: 39.52 ppm; $CDCl_3$: ^{1}H: 7.26 ppm, ^{13}C: 77.16) as an internal reference. Multiplicities are reported as follows: s = singlet, d = doublet, t = triplet, q = quadruplet, m = multiplet, bs = broad singlet. Mass spectra were measured on a Microtof-Q Bruker Daltonics spectrometer coupled with a LC equipment (U3000 Thermofisher). Analytical RP-HPLC was performed on a Welch XB-C18 column (4.6 x 250 mm, 5 µm) running linear gradients CH_3CN (30-70%) into H_2O (0.1% TFA, v/v) over 60 min at 1 mL/min flow rate, with UV detection at 221 nm. Semi-preparative RP-HPLC purification was done on an YMC-Pack ODS-A (10x 250 mm, 5µm) running linear gradients of CH_3CN into H_2O (0.1% TFA, v/v) as indicated for each peptide, at a flow rate of 2 mL/min.

β,γ-Diamino Acids Synthesis. *Cbz-(β,γ)-DiAA(β-Boc)-OCH₃* (Compound **7**, **8**, **9** and **10**). Compound **7**, **8**, **9** and **10** were synthesized from Cbz-D-Phenylalanine or L-Phenylalanine, according the previously described procedure.[23,43]

Fmoc-(β,γ)-DiAA(β-Boc)-OH (Compound **3**, **4**,[43] **5**, and **6**). A solution of Cbz-(β,γ)-DiAA(β-Boc)-OCH_3 (1.0 equiv.) and LiOH.H_2O (10 equiv., 0.5 N final conc.) in a mixture of THF/water (2/1, v/v) was stirred for 2 h at rt. After volatile removal, the aqueous layer was acidified with 2N aqueous hydrochloric acid to pH 1 and then extracted with ethyl acetate. The combined organic layers were washed with water, dried with anhydrous $MgSO_4$, filtered and concentrated under reduced pressure to afford a white solid that was used without any further purification.

A solution of previously saponified compound (1.0 equiv.) in dry MeOH (100 mg/mL) was stirred for 30 min in the presence of 10 wt. % Pd/C (10 mol %) at rt under H_2 (1 bar). Filtration of the catalyst through celite pad and concentration under reduced pressure gave a white solid in quantitative yield.

To a stirred solution of the hydrogenated compound (1.0 equiv.) in a mixture of water/dioxane (50 mg/mL, 1/1, v/v) was added FmocOSu (1.3 equiv.) and K_2CO_3 (5 equiv.). The resulting mixture was allowed to stir for 15 h at rt. After extraction with diethyl ether to remove the excess of FmocOSu, it was acidified with 2N aqueous hydrochloric acid to pH 1 and extracted with ethyl acetate. The combined organic layers were washed with water, dried with anhydrous $MgSO_4$, filtered and concentrated under reduced pressure to afford a white solid. Crude compound **3** and **5** were purified by chromatography (SiO_2, DCM/MeOH, 97/3, v/v). Compound **4** and **6** was washed with diethyl ether to remove the residue of FmocOsu. Compound **3**, **4**, **5** and **6** were all obtained in reasonable yields: 39%, 84%, 35% and 85%, respectively.

Fmoc-(β,γ)-DiAA(β-Alloc)-OH (Compound **5a** and **6a**). A solution of **5** or **6** in a mixture of TFA/DCM (100 mg/mL, 1/1, v/v) was stirred for 1 h at rt. After volatile removal, the residue was dissolved in a mixture of water/dioxane (50 mg/mL, 1/1, v/v) followed by addition of AllocOSu (1.3 equiv) and Na_2CO_3 (1.0 equiv). The resulting mixture was allowed to stir for 15 h at rt. After extraction with diethyl ether to remove the excess of AllocOSu, it was acidified with 2N aqueous hydrochloric acid to pH 1 and then extracted with ethyl acetate. The combined organic layers were washed with water, dried with anhydrous $MgSO_4$, filtered and concentrated under reduced pressure to afford a crude product. The crude product was purified by chromatography (SiO_2, DCM/MeOH, 97/3, v/v) to deliver a white solid. The yields of compounds **5a** and **6a** are 54% and 69%, respectively.

Compound **3** or **5**. ^{1}H NMR (600 MHz, DMSO): δ 11.74 (bs, 1H), 7.89 (d, J = 7.5 Hz, 2H), 7.64 (d, J = 6.9 Hz, 2H), 7.43-7.40 (m, 2H), 7.35-7.31 (m, 3H), 7.24-7.19 (m, 4H), 7.16-7.14 (m, 1H), 6.78 (d, J = 5.8 Hz, 1H), 4.22-4.11 (m, 3H), 4.04-3.98 (m, 1H), 3.94-3.87(m, 1H), 2.79-2.76 (m, 1H), 2.62-2.58 (m, 1H), 2.45-2.28 (m, 2H),1.42 (s, 9H). ^{13}C NMR (150 MHz, DMSO): δ 171.3, 156.8, 156.1, 144.9, 144.8, 141.7, 140.0, 130.0, 129.0, 128.6, 128.0, 126.9, 126.2, 121.1, 121.0, 78.8, 66.2, 56.6, 52.6, 47.7, 37.7, 37.3, 29.2. MS: (ESI+): *m/z*: calcd for $C_{31}H_{34}N_2NaO_6^+$: 553.23 $[M+Na]^+$; found: 553.25.

Compound **4** or **6**. ^{1}H NMR (600 MHz, DMSO): δ 12.03 (bs, 1H),7.87 (dd, J_1 = 3.6 Hz, J_2= 7.8 Hz, 2H), 7.61 (d, J = 7.6 Hz, 2H), 7.42-7.38 (m, 2H), 7.35-7.28 (m, 3H), 7.25-7.18 (m, 4H), 7.13-7.10 (m, 1H), 6.94 (d, J = 9.2 Hz, 1H), 4.17-4.07 (m, 3H), 3.97-3.89 (m, 1H), 3.78-3.73 (m, 1H), 2.87 (dd, J_1 = 2.8 Hz, J_2= 14.3 Hz, 1H), 2.60 (dd, J_1 = 11.4 Hz, J_2 = 14.3 Hz, 1H), 2.47 (dd, J_1 = 3.8 Hz, J_2 = 15.6 Hz, 1H), 2.35 (dd, J_1 = 9.7 Hz, J_2 = 15.6 Hz, 1H),1.40 (s, 9H). ^{13}C NMR (150 MHz, DMSO): δ 173.8, 156.8, 156.2, 144.9, 144.7, 141.6, 140.3, 130.1, 128.9, 128.6, 128.0, 126.8, 126.2, 121.1, 121.0, 78.6, 66.2, 56.8, 52.6, 47.7, 37.7, 37.3, 29.2. MS: (ESI+): *m/z*: calcd for $C_{31}H_{34}N_2NaO_6^+$: 553.23 $[M+Na]^+$; found: 553.08.

Compound **5a**. ^{1}H NMR (600 MHz, DMSO): δ 12.15 (bs, 1H), 7.89 (d, J = 7.4 Hz, 2H), 7.64-7.61 (m, 2H), 7.43-7.39 (m, 2H), 7.36-7.30 (m, 2H), 7.27-7.20 (m, 5H), 7.18-7.12 (m, 2H), 5.98-5.91 (m, 1H), 5.33 (d, J = 17.4 Hz, 1H), 5.20 (d, J = 10.5 Hz, 1H), 4.55-4.49 (m, 2H), 4.22-4.16 (m, 2H), 4.14-4.07 (m, 2H), 3.94-3.85 (m, 1H), 2.87-2.75 (m, 1H), 2.63-2.59 (m, 1H), 2.51-2.47 (m, 1H), 2.41-2.33 (m, 1H). ^{13}C NMR (150 MHz, DMSO): δ 172.8, 156.3, 156.0, 144.3, 141.1, 139.3, 134.2, 129.5, 128.5, 128.1, 127.5, 126.5, 125.7, 120.6, 117.3, 65.9, 64.8, 55.7, 51.4, 47.1, 37.5, 36.9. MS: (ESI+): *m/z*: calcd for $C_{30}H_{31}N_2O_6^+$: 515.22 $[M+H]^+$; found: 514.92.

Compound **6a**. ^{1}H NMR (600 MHz, DMSO): δ 12.15 (bs, 1H), 7.88-7.87 (m, 2H), 7.62 (d, J = 7.2 Hz, 2H), 7.43-7.38 (m, 4H), 7.34-7.29 (m, 2H), 7.27-7.20 (m, 4H), 7.14-7.12 (m, 1H), 5.96-5.90 (m, 1H), 5.32 (d, J = 17.2 Hz, 1H), 5.18 (d, J = 10.3 Hz, 1H), 4.51 (d, J = 4.68 Hz, 2H), 4.19-4.08 (m, 3H), 4.04-3.98 (m, 1H), 3.80-3.75 (m, 1H), 2.88-2.85 (m, 1H), 2.64-2.60 (m, 1H), 2.53-2.49 (m, 1H), 2.40-2.36 (m, 1H). ^{13}C NMR (150 MHz, DMSO): δ 173.2, 156.3, 156.1, 144.3, 144.2, 141.1, 139.6, 134.3, 129.6, 128.4, 128.1, 127.5, 126.3, 125.8, 120.5, 117.2, 65.7, 64.7, 56.2, 52.5, 47.2, 37.1, 36.7. MS: (ESI+): *m/z*: calcd for $C_{30}H_{31}N_2O_6^+$: 515.22 $[M+H]^+$; found: 514.92.

Peptide Synthesis. Peptide length elongation was started from Fmoc-Pro-(2-CTC)–Resin, either by Manual Peptide Synthesis or Automated Peptide Synthesis.

Manual Peptide Synthesis. The manual peptide synthesis was performed using the following protocol:

(1) Swelling in DMF for 20 min

(2) 2× cleavage of the Fmoc protection group with 20% piperidine in DMF for 15 min

(3) washing sequentially with DMFx 2, MeOHx 2, DCMx 2, DMF

(4) Coupling with Fmoc-AA-OH (4.0 equiv), HOBt (4.0 equiv), HBTU (4.0 equiv), and DIPEA (8.0 equiv) in DMF for 60 min

(5) washing sequentially with DMFx 2, MeOHx 2, DCMx 2, DMF

Steps 2−5 were performed as long as the peptides were completely assembled.

Automated Peptide Synthesis. Peptides were synthesized by a microwave-assisted peptide synthesizer (Discovery Bio, CEM) using the following cycles of deprotection, coupling and washing.

(1) Fmoc deprotection: T = 50 °C, Δ_T = 1 °C, $P_{microwave}$ = 30 W, t = 210 s with 20% piperidine in DMF, 4 mL/deprotection.

(2) Peptide Coupling: T = 50 °C, Δ_T = 1 °C, $P_{microwave}$ = 30 W, t = 600 s with Fmoc-AA-OH (5 equiv.), HBTU (5 equiv.) and DiPEA (0.3 M in DMF, 12 equiv., 4 mL/coupling)

(3) Washing: after each deprotection or coupling, resin was washed with DMFx 3 (3 mL/time).

Resin Cleavage. Resin cleavage was performed with 1% TFA in DCM (5x 10 min) to keep the side-chain protecting groups untouched. After cleavage, the product solution was coevaporated with toluene (1/1, v/v) to give the side-chain-protected linear peptides as a solid which was used without any further purification.

Peptide Cyclization. To a solution of linear peptide in DMF (2 mL/mg) was added PyBOP (5.0 equiv.), HOBt (5.0 equiv.) and DiPEA (15.0 equiv.). After stirred for 15 h at rt, the solvent was removed under reduced pressure.

Global Deprotection and Precipitation. The crude cyclized peptide was dissolved in TFA/water (9/1, v/v, 10 mg/mL) and allowed to stir for 1 h at rt. After evaporation of the TFA/water from the global deprotection, equal volume (0.5 mL) aliquots of TFA solution were poured into two 15 mL conical tubes. Cold diethyl ether (14 mL) was then dumped into each conical tube. Precipitation was observed immediately and let for incubation for another 15 min in ice bath. Precipitate was pelleted by centrifugation (3000 rpm, 15 min) and transferred to round flask after removal of the ether supernatant. Purification by semi-preparative RP-HPLC and lyophilization gave the GS and analogues as a white powder.

cyclo(Pro-^{D}Phe-Leu-Orn-Val-)$_2$ (GS). GS was synthesized using Manual Peptide Synthesis on a 0.25 mM scale (57 mg, 0.050 mmol, 20% overall yield, 98% purity). Analytic RP-HPLC, linear 30-70% CH_3CN (0.1% TFA) gradient into H_2O (0.1% TFA) for 60 min. Detections were done at 221 nm using a photodiode array detector. t_r = 47.88 min; MS: (ESI+): *m/z*: 571.33 $[M+2H]^{2+}$, 1141.42 $[M+H]^+$; for NMR data see Tables S1 in the Supporting Information.

*cyclo(Pro-^{D}Phe-Leu-Orn-Val-(βR,γR)-DiAA-Leu-Orn-Val-) (GS**3**)*. GS**3** was synthesized using Manual Peptide Synthesis on a 0.25 mM scale (30 mg, 0.028 mmol, 11% overall yield, 96% purity). Analytic RP-HPLC, linear 30-70% CH_3CN (0.1% TFA) gradient into H_2O (0.1% TFA) for 60 min. Detections were done at 221 nm using a photodiode array detector. t_r = 18.13 min; MS: (ESI+): *m/z*: 544.33 $[M+2H]^{2+}$, 1087.33 $[M+H]^+$; for NMR data see Tables S1 in the Supporting Information.

*cyclo(Pro-^{D}Phe-Leu-Orn-Val-(βS,γR)-DiAA-Leu-Orn-Val-) (GS**4**)*. GS**4** was synthesized using Manual Peptide Synthesis on a 0.25 mM scale (45 mg, 0.041 mmol, 17% overall yield, 99% purity). Analytic RP-HPLC, linear 30-70% CH_3CN (0.1% TFA) gradient into H_2O (0.1% TFA) for 60 min. Detections were done at 221 nm using a photodiode array detector. t_r = 21.76 min; MS: (ESI+): *m/z*: 544.25 $[M+2H]^{2+}$, 1087.33 $[M+H]^+$, 1109.42 $[M+Na]^+$; for NMR data see Tables S1 in the Supporting Information.

*cyclo(Pro-^{D}Phe-Leu-Orn-Val-(βS,γS)-DiAA-Leu-Orn-Val-) (GS**5**)*. GS**5** was synthesized using Manual Peptide Synthesis on a 0.25 mM scale (43 mg, 0.040 mmol, 16% overall yield, 95% purity). Analytic RP-HPLC, linear 30-70% CH_3CN (0.1% TFA) gradient into H_2O (0.1% TFA) for 60 min. Detections were done at 221 nm using a photodiode array detector. t_r = 20.82 min; MS: (ESI+): *m/z*: 544.25 $[M+2H]^{2+}$, 1087.25 $[M+H]^+$ 1109.33 $[M+Na]^+$; for NMR data see Tables S1 in the Supporting Information.

*cyclo(Pro-^{D}Phe-Leu-Orn-Val-(βR,γS)-DiAA-Leu-Orn-Val-) (GS**6**)*. GS**6** was synthesized using Manual Peptide Synthesis on a 0.25 mM scale (27 mg, 0.025 mmol, 10% overall yield, 99% purity). Analytic RP-HPLC, linear 30-70% CH_3CN (0.1% TFA) gradient into H_2O (0.1% TFA) for 60 min. Detections were done at 221 nm using a photodiode array detector. t_r = 20.73 min; MS: (ESI+): *m/z*: 544.33 $[M+2H]^{2+}$, 1087.42 $[M+H]^+$ 1109.50 $[M+Na]^+$; for NMR data see Tables S1 in the Supporting Information.

*cyclo(Pro-^{D}Phe-Leu-Orn-Val-(βS,γS)-DiAA(β-Lys)-Leu-Orn-Val-) (GS**5K**)*. GS**5K** was synthesized using Automated Peptide Synthesis on a 0.1 mM scale (21 mg, 0.017 mmol, 17% overall yield, 93% purity). Analytic RP-HPLC, linear 30-70% CH_3CN (0.1% TFA) gradient into H_2O (0.1% TFA) for 60 min. Detections were done at 221 nm using a photodiode array detector. t_r = 16.43 min; MS: (ESI+): *m/z*: 608.42 $[M+2H]^{2+}$, 1215.42 $[M+H]^+$; for NMR data see Tables S1 in the Supporting Information.

*cyclo(Pro-^{D}Phe-Leu-Orn-Val-(βS,γS)-DiAA(β-Phe)-Leu-Orn-Val-) (GS**5F**)*. GS**5F** was synthesized using Automated Peptide Synthesis on a 0.1 mM scale (15 mg, 0.012 mmol, 12% overall yield, 91% purity). Analytic RP-HPLC, linear 30-70% CH_3CN (0.1% TFA) gradient into H_2O (0.1% TFA) for 60 min. Detections were done at 221 nm using a photodiode array detector. t_r = 22.24 min; MS: (ESI+): *m/z*: 618.08 $[M+2H]^{2+}$, 1234.58 $[M+H]^+$; for NMR data see Tables S1 in the Supporting Information.

*cyclo(Pro-^{D}Phe-Leu-Orn-Val-(βR,γS)-DiAA(β-Lys)-Leu-Orn-Val-) (GS**6K**)*. GS**6K** was synthesized using Automated Peptide Synthesis on a 0.1 mM scale (38 mg, 0.031 mmol, 31% overall yield, 97% purity). Analytic RP-HPLC, linear 30-70% CH_3CN (0.1% TFA) gradient into H_2O (0.1% TFA) for 60 min. Detections were done at 221 nm using a photodiode array detector. t_r = 17.40 min; MS: (ESI+): *m/z*: 608.42 $[M+2H]^{2+}$, 1215.67 $[M+H]^+$; for NMR data see Tables S1 in the Supporting Information.

*cyclo(Pro-^{D}Phe-Leu-Orn-Val-(βR,γS)-DiAA(β-Phe)-Leu-Orn-Val-) (GS**6F**)*. GS**6F** was synthesized using Automated Peptide Synthesis on a 0.1 mM scale (15 mg, 0.012 mmol, 12% overall yield, 92% purity). Analytic RP-HPLC, linear 30-70% CH_3CN (0.1% TFA) gradient into H_2O (0.1% TFA) for 60 min. Detections were done at 221 nm using a photodiode array detector. t_r = 27.01 min; MS: (ESI+): *m/z*: 618.00 $[M+2H]^{2+}$, 1234.67 $[M+H]^+$; for NMR data see Tables S1 in the Supporting Information.

NMR Spectroscopy. The NMR samples contained GS (2 mM) or GS**3**-**6** (10 mM) were dissolved in 0.5 mL of H_2O/D_2O (9/1, v/v, containing 20 mM PBS buffer) at pH 7.0. The rest of GS analogues were prepared at 10-20 mM peptide concentration in 0.5 mL of DMSO-d_6. NMR spectra were acquired on a Bruker AV 500 or 600 MHz spectrometer at 4 °C or 25 °C. ^{1}H, COSY, TOCSY and NOESY spectroscopies were recorded to fully assign the cyclic peptides complex data. Spectra were acquired by standard pulse sequences using presaturation of the water signal if necessary. The mixing times for TOCSY and NOESY are 80 ms and 500 ms, respectively.

Circular Dichroism Spectroscopy. Samples for CD spectra were prepared at 0.1 mM solutions in water or methanol. All spectra were measured on a MOS-450 Spectrometer using a circular quartz cell with a path length of 1 cm at 25 °C. Spectra were documented with a band width of 1 nm, a duration time of 1 s and a scan speed of 100 nm/min. Molar ellipticity [θ] was used to evaluate the Cotton effect. Each measurement was repeated 3 times to calculate the mean value. The spectra from solvents were subtracted as background in data analysis.

Antibacterial Assay. The following bacterial strains were used: *Escherichia coli* (ATCC 25922), *Pseudomonas aeruginosa* (ATCC 27853), *Staphylococcus aureus* (ATCC 29213), *Bacillus subtilis* (ATCC 6633), *Streptococcus bovis* (ATCC 33317), *Enterococcus faecalis* (ATCC 29212) and *Enterococcus faecium* (ATCC 35667). All culture media used for bacteria incubation were freshly prepared. Bacteria were grown at Tryptic Soy Broth (TSB) under constant shaking at 200 rpm for 6 h to mid-logarithmic phase and harvested by centrifugation (10000x g for 3 min). The cells were washed three times with PBS buffer (10 mM, pH 7.4) and resuspended to A_{620} 0.02 in TSB broth. GS and GS analogues were dissolved in DMSO at 1 mg/mL as stock solution (2 mg/L solution was used for *P. aeruginosa*). The stock solution was diluted in DMSO to obtain a series of 2-fold dilutions. 96 Microtiter wells were filled with 10 µL (5 µL for *P. aeruginosa*) GS or GS analogues solution in DMSO and 90 µL (95 µL for *P. aeruginosa*) suspension of a mid-logarithmic phase culture of bacteria. Cultures were carried out in triplicate. DMSO was used as negative control. The MICs were assessed by measuring turbidity at 620 nm after 48 h incubation at 37 ºC. The 620 nm absorbance was measured on a Multiskan FC microplate reader (Thermo Scientific).

Hemolysis Assay. Human blood solution, 10% (w/v) SDS solution and PBS (10 mM, pH 7.4) solution were freshly prepared.GS and GS analogues were dissolved in DMSO at 10 mg/mL as stock solution. The stock solution was diluted in DMSO to obtain a series of 2-fold dilutions. Fresh human blood solution was diluted to $5x10^5$ erythrocytes per milliliter. For each well, 5 µL peptide, 45 µL PBS solution and 50 µL diluted blood solution was added. DMSO was used as negative control. SDS (0.1% w/v final concentration) was used as 100% hemolysis control. Cultures were carried out in triplicate and incubated for 30 min at 37 ºC. Erythrocytes were separated by centrifugation (300 rpm, 10 min). A volume of 50 µL portion of each supernatant was transferred to a new 96 microtiter plate to measure the turbidity at 450 nm.

Cytotoxicity Assay. Peptides were dissolved in DMSO at 2.5 mM as stock solution. The stock solution was diluted in cell medium (RPMI 1640, containing 100 U penicillin and 100 µg/mL streptomycin) supplemented with 1% fetal bovine serum to obtain a series of dilutions (0.1, 1, 5, 10 or 25 µM). LO2 cells were applied in this work and were cultured in cell medium supplemented with 1% fetal bovine serum in a humidified incubator at 37 ºC in 5% CO_2. The cells ($5 x10^3$ cells per well) were seeded in a 96-well plate in cell medium overnight. After culture medium removal, 100 µL medium containing different concentrations of peptide was added. Cultures were carried out in triplicate. After incubation for 24 h, the culture medium was removed, 100 µL fresh CCK-8 medium (90 µL cell medium and 10 µL CCK-8 solution) (Medchem Express, USA) was added to each well and the samples were incubated for another 2 h. The absorbance at 450 nm was measured by a SpectraMax i3x microplate reader (MD, USA).

Cytoplasmic Membrane Depolarization. *S. aureus* and *B. subtilis* were grown at Luria Bertani (LB) broth under constant shaking at 200 rpm for 6 h to mid-logarithmic phase and harvested by centrifugation (10000x g for 3 min). The cells were washed three times with wash buffer (5 mM HEPES, 20 mM glucose, pH 7.4) and resuspended to A_{620} 0.005 (*S. aureus*) or A_{620} 0.03 (*B. subtilis*) in the same buffer. Then, 0.1 M KCl was added to equilibrate the cytoplasmic and external K concentration. A volume of 2 mL of cell suspension was placed in a 1 cm cuvette followed by the addition of a $DiSC_3$-5 stock solution (4 mM in HEPES buffer) to a final concentration of 200 nM. The resulting solution was incubated until a stable reduction of fluorescence was achieved, indicating the successful uptake of the dye into the bacterial membrane. Changes in fluorescence were recorded with a CaryEclipse fluorescence spectrophotometer (Aginent, USA). After the addition of peptides (2x MIC), membrane depolarization was determined by monitoring the change in fluorescence emission intensity of the $DiSC_3$-5 dye at excitation and emission wavelengths of 622 and 670 nm, respectively. The addition of gramicidin S (4x MIC) was used to achieve maximum fluorescence.

Scanning Electron Microscopy. Pathogens were grown at TSB broth under constant shaking at 200 rpm for 6 h to mid-logarithmic phase and harvested by centrifugation (10000x g for 3 min). The cells were washed three times with PBS buffer (10 mM, pH 7.4) and resuspended to A_{620} 0.4 in the same medium. Peptide treatment of the bacterial cells was carried out at 37 ºC for 1 h at their respective 2x MICs. Bacteria incubated with PBS served as the control. After the incubation, the cells were harvested by centrifugation (8000x g for 5min) and washed with PBS three times. Bacterial cells were then fixed with 2.5% (w/v) glutaraldehyde at 4 ºC for 6 h. Before centrifugation at 8000x g for 3min, the cells were mixed by gently inverting the tube up and down for several minutes to prevent clumping of the cells. After three washes with PBS, the bacterial pellets were dehydrated for 15 min with a series of graded ethanol solutions (30, 50, 70, 80, 90 and 100%), the cells were mixed and centrifuged at 8000x g for 3 min. Following dehydration, the dried bacterial cells were transferred to dry alcohol. A volume of 10 uL of cell suspension was transferred to the cover slide and allowed to oven-dried at 60 ºC for 5 min. The slides were coated and visualized under a scanning electron microscope (FEI Field Electron Microscope, Quanta 250, USA).

Acknowledgements

This work was financially supported by the National Natural Science Foundation of China (No. 21967012), Health and Family Planning Commission of Jiangxi Province (20195647,2018B012), start-up grant (No. 2018BSZR007) from Jiaxngxi University of Traditionnal Chinese Medicine and State Key Laboratory for Chemistry and Molecular Engineering of Medicinal Resources (Guangxi Normal University, CMEMR2019-B07). We thank Dr. Jingxian Yu (The University of Adelaide, Australia) for attempted DFT calculations.

Keywords: antimicrobial peptide • gramicidin S • membrane disruption • hemolysis • β,γ-diamino acids

[1] [1] L. Czaplewski, R. Bax, M. Clokie, M. Dawson, H. Fairhead, V. A. Fischetti, S. Foster, B. F. Gilmore, R. E. W. Hancock, D. Harper, I. R. Henderson, K. Hilpert, B. V. Jones, A. Kadioglu, D.Knowles, S. Ólafsdóttir, D. Payne, S. Projan, S. Shaunak, J. Silverman, C. M. Thomas, T. J. Trust, P. Warn, J. H. Rex, *Lancet Infect. Dis.* **2016**, *16*, 239–251.

[2] European Centre for Disease Prevention and Control, *Antimicrobial resistance surveillance in Europe 2015, Annual report of the European Antimicrobial Resistance Surveillance Network (EARS-Net), 2017*

[3] D. A. Goff, R. Kullar, E. J. C. Goldstein, M. Gilchrist, D. Nathwani, A. C. Cheng, K. A. Cairns, K. Escandón-Vargas, M. V. Villegas, A. Brink, D, van den Bergh, M. Mendelson, *Lancet Infect. Dis.* **2017**, *17*, e56–e63.

[4] M. A. Cooper, D. Shlaes, *Nature* **2011**, *472*, 32–32.

[5] M. Mahlapuu, J. Håkansson, L. Ringstad, C. Björn, *Front. Cell. Infect. Microbiol.* **2016**, *6*, 194.

[6] A. L. Llamas-Saiz, G. M. Grotenbreg, M. Overhand, M. J. van Raaij, *Acta Crystallogr. D Biol. Crystallogr.* **2007**, *63*, 401–407.

[7] S. E. Hull, R. Karlsson, P. Main, M. M. Woolfson, E. J. Dodson, *Nature* **1978**, *275*, 206–207.

[8] A. Asano, M. Doi, *X-Ray Struct. Anal. Online* **2019**, *35*, 1–2.

[9] K. Yamada, M. Unno, K. Kobayashi, H. Oku, H. Yamamura, S. Araki, H. Matsumoto, R. Katakai, M. Kawai, *J. Am. Chem. Soc.* **2002**, *124*, 12684–12688.

[10] G. G. Gause, M. G. Brazhnikova, *Nature* **1944**, *154*, 703.

[11] S. Afonin, U. H. N. Dürr, P. Wadhwani, J. Salgado, A. S. Ulrich, in *Bioact. Conform. II* (Ed.: T. Peters), Springer Berlin Heidelberg, Berlin, Heidelberg, **2008**, pp. 139–154.

[12] Md. Ashrafuzzaman, O. S. Andersen, R. N. McElhaney, *Biochim. Biophys. Acta BBA - Biomembr.* **2008**, *1778*, 2814–2822.

[13] M. Wenzel, M. Rautenbach, J. A. Vosloo, T. Siersma, C. H. M. Aisenbrey, E. Zaitseva, W. E. Laubscher, W. van Rensburg, J. C. Behrends, B. Bechinger, L. W. Hamoena, *mBio* **2018**, *9*, e00802-18.

[14] T. Katsu, T. Imamura, K. Komagoe, K. Masuda, T. Mizushima, *Anal. Sci.* **2007**, *23*, 517–522.

[15] M. Wenzel, A. I. Chiriac, A. Otto, D. Zweytick, C. May, C. Schumacher, R. Gust, H. B. Albada, M. Penkova, U. Krämer, R. Erdmannj, N. Metzler-Nolteh, S. K. Strausk, E. Bremerl, D.Becherc, H. Brötz-Oesterheltf, H. Sahlb, J. E. Bandowa, *Proc. Natl. Acad. Sci.* **2014**, *111*, E1409–E1418.

[16] M. Berditsch, S. Afonin, J. Reuster, H. Lux, K. Schkolin, O. Babii, D. S. Radchenko, I. Abdullah, N. William, V. Middel, U. Strähle, A. Nelson, K. Valko, A. S. Ulrich, *Sci. Rep.* **2019**, *9*, 1–15.

[17] L. H. Kondejewski, S. W. Farmer, D. S. Wishart, R. E. w. Hancock, R. S. Hodges, *Int. J. Pept. Protein Res.* **1996**, *47*, 460–466.

[18] Q. Guan, S. Huang, Y. Jin, R. Campagne, V. Alezra, Y. Wan, *J. Med. Chem.* **2019**, *62*, 7603–7617.

[19] S. Pal, U. Ghosh, R. S. Ampapathi, T. K. Chakraborty, in *Pept. II* (Ed.: W. Lubell), Springer International Publishing, Cham, **2015**, pp. 159–202.

[20] A. D. Knijnenburg, E. Spalburg, A. J. de Neeling, R. H. Mars‐Groenendijk, D. Noort, G. M. Grotenbreg, G. A. van der Marel, H. S. Overkleeft, M. Overhand, *Helv. Chim. Acta* **2012**, *95*, 2544–2561.

[21] M. Jelokhani-Niaraki, L. H. Kondejewski, L. C. Wheaton, R. S. Hodges, *J. Med. Chem.* **2009**, *52*, 2090–2097.

[22] M. Tamaki, I. Sasaki, M. Kokuno, M. Shindo, M. Kimura, Y. Uchida, *Org. Biomol. Chem.* **2010**, *8*, 1791.

[23] Y. Wan, A. Stanovych, D. Gori, S. Zirah, C. Kouklovsky, V. Alezra, *Eur. J. Med. Chem.* **2018**, *149*, 122–128.

[24] A. S. Kotmale, E. Sangtani, R. G. Gonnade, D. Sarkar, S. Burade, P. R. Rajamohanan, G. J. Sanjayan, *New J. Chem.* **2018**, *42*, 1197–1201.

[25] S. Pal, G. Singh, S. Singh, J. K. Tripathi, J. K. Ghosh, S. Sinha, R. S. Ampapathi, T. K. Chakraborty, *Org. Biomol. Chem.* **2015**, *13*, 6789–6802.

[26] B. Legrand, L. Mathieu, A. Lebrun, S. Andriamanarivo, V. Lisowski, N. Masurier, S. Zirah, Y. K. Kang, J. Martinez, L. T. Maillard, *Chem. – Eur. J.* **2014**, *20*, 6713–6720.

[27] A. D. Knijnenburg, A. W. Tuin, E. Spalburg, A. J. de Neeling, R. H. Mars-Groenendijk, D. Noort, J. M. Otero, A. L. Llamas-Saiz, M. J. van Raaij, G. A. van der Marel, H. S. Overkleeft, M. Overhand, *Chem. – Eur. J.* **2011**, *17*, 3995–4004.

[28] C. Priem, A. Wuttke, M. Berditsch, A. S. Ulrich, A. Geyer, *J. Org. Chem.* **2017**, *82*, 12366–12376.

[29] G. Singh, S. Azmi, J. K. Ghosh, R. S. Ampapathi, S. Pal, *ChemistrySelect* **2018**, *3*, 2272–2276.

[30] K. Yamada, S. Shinoda, H. Oku, K. Komagoe, T. Katsu, R. Katakai, *J. Med. Chem.* **2006**, *49*, 7592–7595.

[31] V. V. Kapoerchan, A. D. Knijnenburg, P. Keizer, E. Spalburg, A. J. de Neeling, R. H. Mars-Groenendijk, D. Noort, J. M. Otero, A. L. Llamas-Saiz, M. J. van Raaij, G. A. van der Marel, H. S. Overkleeft, M. Overhand, *Bioorg. Med. Chem.* **2012**, *20*, 6059–6062.

[32] M. Tamaki, T. Harada, K. Fujinuma, K. Takanashi, M. Shindo, M. Kimura, Y. Uchida, *Chem. Pharm. Bull. (Tokyo)* **2012**, *60*, 1134–1138.

[33] O. Babii, S. Afonin, M. Berditsch, S. Reisser, P. K. Mykhailiuk, V. S. Kubyshkin, T. Steinbrecher, A. S. Ulrich, I. V. Komarov, *Angew. Chem.-Int. Ed.* **2014**, *53*, 3392–3395; *Angew. Chem.* **2014**, *53*, 3392–3395.

[34] Y. Q. Yeoh, J. Yu, S. W. Polyak, J. R. Horsley, A. D. Abell, *ChemBioChem* **2018**, *19*, 2591–2597.

[35] O. Babii, S. Afonin, A. Yu. Ishchenko, T. Schober, A. O. Negelia, G. M. Tolstanova, L. V. Garmanchuk, L. I. Ostapchenko, I. V. Komarov, A. S. Ulrich, *J. Med. Chem.* **2018**, *61*, 10793–10813.

[36] C. Solanas, B. G. de la Torre, M. Fernández-Reyes, C. M. Santiveri, M. Á. Jiménez, L. Rivas, A. I. Jiménez, D. Andreu, C. Cativiela, *J. Med. Chem.* **2009**, *52*, 664–674.

[37] C. Solanas, B. G. de la Torre, M. Fernández-Reyes, C. M. Santiveri, M. Á. Jiménez, L. Rivas, A. I. Jiménez, D. Andreu, C. Cativiela, *J. Med. Chem.* **2010**, *53*, 4119–4129.

[38] M. Tamaki, K. Fujinuma, T. Harada, K. Takanashi, M. Shindo, M. Kimura, Y. Uchida, *Bioorg. Med. Chem. Lett.* **2012**, *22*, 106–109.

[39] G. M. Grotenbreg, A. E. M. Buizert, A. L. Llamas-Saiz, E. Spalburg, P. A. V. van Hooft, A. J. de Neeling, D. Noort, M. J. van Raaij, G. A. van der Marel, H. S. Overkleeft, M. Overhand, *J. Am. Chem. Soc.* **2006**, *128*, 7559–7565.

[40] S. Thétiot-Laurent, F. Bouillère, J.-P. Baltaze, F. Brisset, D. Feytens, C. Kouklovsky, E. Miclet, V. Alezra, *Org. Biomol. Chem.* **2012**, *10*, 9660–9663.

[41] A. Stanovych, R. Guillot, C. Kouklovsky, E. Miclet, V. Alezra, *Amino Acids* **2014**, *46*, 2753–2757.

[42] C. T. Hoang, F. Bouillère, S. Johannesen, A. Zulauf, C. Panel, A. Pouilhès, D. Gori, V. Alezra, C. Kouklovsky, *J. Org. Chem.* **2009**, *74*, 4177–4187.

[43] N. Auberger, A. Stanovych, S. Thétiot-Laurent, R. Guillot, C. Kouklovsky, S. C. des Combes, C. Pacaud, I. Devillers, V. Alezra, *Amino Acids* **2016**, *48*, 2237–2242.

[44] M. Tamaki, S. Akabori, I. Muramatsu, *J. Am. Chem. Soc.* **1993**, *115*, 10492–10496.

[45] Y. Wan, J.-P. Baltaze, C. Kouklovsky, E. Miclet, V. Alezra, *J. Pept. Sci.* **2019**, *25*, e3143.

[46] D. S. Wishart, B. D. Sykes, F. M. Richards, *Biochemistry* **1992**, *31*, 1647–1651.

[47] L. H. Kondejewski, S. W. Farmer, D. S. Wishart, C. M. Kay, R. E. W. Hancock, R. S. Hodges, *J. Biol. Chem.* **1996**, *271*, 25261–25268.

[48] L. H. Kondejewski, M. Jelokhani-Niaraki, S. W. Farmer, B. Lix, C. M. Kay, B. D. Sykes, R. E. W. Hancock, R. S. Hodges, *J. Biol. Chem.* **1999**, *274*, 13181–13192.

[49] V. V. Kapoerchan, A. D. Knijnenburg, M. Niamat, E. Spalburg, A. J. de Neeling, P. H. Nibbering, R. H. Mars-Groenendijk, D. Noort, J. M. Otero, A. L. Llamas-Saiz, M. J. van Raaij, G. A. van der Marel, H. S. Overkleeft, M. Overhand, *Chem. – Eur. J.* **2010**, *16*, 12174–12181.

[50] M. Kawai, H. Yamamura, R. Tanaka, H. Umemoto, C. Ohmizo, S. Higuchi, T. Katsu, *J. Pept. Res.* **2004**, *65*, 98–104.

[51] M. R. Yeaman, N. Y. Yount, *Pharmacol. Rev.* **2003**, *55*, 27–5